KSCE Journal of Civil Engineering (2019) 23(5):2281-2292
Copyright ⓒ2019 Korean Society of Civil Engineers
DOI 10.1007/s12205-019-1313-6

Structural Engineering

pISSN 1226-7988, eISSN 1976-3808
www.springer.com/12205

Mechanical Performance of Stiffened Concrete Filled Double Skin Steel Tubular Stub Columns under Axial Compression

Hussein Ghanim Hasan* and Talha Ekmekyapar**

Received July 3, 2018/Revised November 15, 2018/Accepted January 15, 2019/Published Online February 11, 2019

Abstract

This paper presents the mechanical performance of Concrete Filled Double Skin Steel Tube (CFDST) columns stiffened by Welded Reinforcing Bars (WRBs) under axial compression. A series of experiments were carried out on sixteen CFDST columns using two different *D*/*t* ratios and different patterns of WRBs as parameters. The steel reinforcing bars were welded either on the external surface of the inner tubes or on the internal surface of the outer tubes. Various patterns were used to enable a better understanding of the stiffened CFDST columns performance. Moreover, the compressive loading vs. end shortening curves, failure modes, strength index and concrete-steel contribution ratio were analysed. The results showed that a certain pattern of the WRBs affords additional ductility and strength capacity of the stiffened CFDST columns. Furthermore, WRBs play an important role in the mitigating failure modes and work consistently with the shell concrete of these columns. Design methods were developed for the calculation of the strength capacity of stiffened CFDST columns and assessed against the experimental results to trace the suitable formulation for design purposes. The outcomes of modified analytical procedures mostly match well with the experimental results of the stiffened CFDST columns.

Keywords: *CFDST columns, welded reinforcing bars, failure modes, experiments, design methods*

1. Introduction

Concrete Filled Steel Tube (CFST) columns have been commonly utilized in the high-rise buildings, subways, bridges and industrial structures owing to their excessive advantages as ductility, high strength, and good seismic behaviour (Aslani *et al.*, 2017; Kim and Shim, 2016; Yang *et al.*, 2017; Zhang *et al.*, 2017). Generally, the concrete delays or averts the steel tube from buckling, and the tube confines the concrete in the CFST members (Aslani *et al.*, 2015b; Aslani *et al.*, 2016; Gopal, 2017; Park *et al.*, 2011). Additionally, the steel hollow section acts as a jacket for concrete, accordingly, provides good confinement and enhances the behaviour. Recently, demand for lighter-weight members increased widely in the world to decrease the dead loads, mainly for multi-story building (Abbas *et al.*, 2017; Aslani *et al.*, 2015a; Elchalakani *et al.*, 2002; Fu *et al.*, 2018; Gopal, 2017). The inventive novelty of composite structure is recognised as Concrete Filled Double Skin Steel Tube (CFDST) column. CFDSTs consider the best solution to decrease the foundation loads due to the void inside the inner tube (Elchalakani *et al.*, 2002; Essopjee and Dundu, 2015; Hassan *et al.*, 2016; Romero *et al.*, 2017). CFDST comprises concrete infill between the two-concentric steel hollow tubes, where the inner tube is empty as shown in Fig. 1. The CFDST column gets equal or higher characteristics than the ordinary CFST column, where the outer tube of CFDST performs as a CFST column, while the inner tube works as an unfilled compact tube (Zhao and Grzebieta, 2002).

Over the last few years, numerous studies were carried out about the imperfect bonding that occurs in the CFST and CFDST columns within an elastic stage (Kwan *et al.*, 2016; Lai and Ho, 2014). This phenomenon happens due to the fact that concrete and steel tubes suffer from deformation with dissimilar rates. The Poisson's ratio of the steel is higher than that of the concrete, and the lateral expansion of concrete is lesser than the steel expansion in this stage (Ekmekyapar *et al.*, 2019). This leads to an unconfined or free the concrete behaviour until the concrete cracks occur. This behaviour postpones the confinement effect and decreases the effectiveness of the steel tube (Kwan *et al.*, 2016). Therefore, recent studies in the literature tend to improve the performance of such columns in the elastic stage by considering different configurations (Essopjee and Dundu, 2015; Hassan *et al.*, 2016; Romero *et al.*, 2017). Moreover, some studies (Ge and Usami, 1992; Lee *et al.*, 2012; Lin *et al.*, 1993; Tao *et al.*, 2005; Tao *et al.*, 2009) have demonstrated the effectiveness of stiffening members to enhance the performance of CFST members, such as longitudinal stiffeners and reinforcing bars. However, the effect of stiffening members in delaying the local buckling of steel tubes have been confirmed by tests (Tao *et al.*,

*Ph.D. Student, Dept. of Civil Engineering, University of Gaziantep, Gaziantep 27310, Turkey (Corresponding Author, E-mail: hussein8ghanim@gmail.com)
**Associate Professor, Dept. of Civil Engineering, University of Gaziantep, Gaziantep 27310, Turkey (E-mail: ekmekyapar@gantep.edu.tr)

2008; Tao *et al.*, 2007). In addition, the stiffening members welded with the steel tube act to enhance the ductility and strength of the CFST columns due to the additional interaction provided (Kwan *et al.*, 2016; Shekastehband *et al.*, 2017). It was also concluded that the role of the stiffening members improves dramatically the fire resistance of the composite columns (Shekastehband *et al.*, 2017). Correspondingly, the welding of the internal stiffening members is possible only with a large diameter of steel tubes, whereas, they are difficult to weld with the steel tubes that have a small diameter (Dong and Ho, 2013; Han *et al.*, 2014).

Many researchers have studied the mechanical performance of the CFDST and CFST columns experimentally and analytically in the previous years. For example, Wei *et al.* (1995) proposed a design formula to estimate the response of the CFDSTs under an axial load up to its peak strength. Elchalakani *et al.* (2018) theoretically and experimentally concluded that the CFDSTs were filled using a rubberised concrete can be used as a new construction technology for applications in seismic zones and security bollards. Hui *et al.* (1998) discussed the failure modes of CFST columns and developed the analytical model for the axial compression. Han *et al.* (2014) reported that the concrete of CFST can change the failure modes of the outer tubes. Dabaon *et al.* (2009), conducted theoretical and experimental tests to explore the performance of stiffened and unstiffened stainless CFST columns. Tao *et al.* (2008) concluded that the strength and ductility of CFST can be increased with increasing the number of stiffening members on the tube surface. Ge and Usami (1992) reported that the CFST columns behaviour can be improved by either welding longitudinal strips on the inner surface of the tube or welding shear studs. Shekastehband *et al.* (2017) investigated the longitudinal steel-stiffening members embedded in the surfaces of tubes of CFDST column improving steel-concrete contact, consequently, improve the fire resistance of the columns.

In view of the literature above, few experimental and analytical studies were undertaken to concentrate on the CFDST columns with stiffening members. Therefore, the behaviour of the stiffened CFDST columns is still obscure. In this context, the aim of the current study is to explore experimentally and analytically the mechanical performance of CFDST columns stiffened by an innovative type of stiffening members, which is described as "welded reinforcing bar" (WRBs). 16 specimens have been tested to assess the impact of the parameters. The main parameters of this work are as follows:

1) Two different patterns of WRBs, the first pattern includes reinforcing bars welded on the external surface of the inner steel tube, whereas the second pattern includes reinforcing bars welded on the internal surface of the outer tubes. The innovative patterns were altered to find out the best position of WRBs within CFDST column, which in turn helps to delay the buckling of tubes and to enhance the confinement effect on sandwiched concrete. Moreover, each pattern includes a different number of WRBs (6, 4 and 3).
2) To be able to explore the effect of tube thicknesses, two different thicknesses of steel tubes were utilized.

Finally, the analytical methods that were proposed by several investigators for unstiffened CFDST columns were developed to estimate the cross-section capacities of stiffened CFDST columns. It is shown in this study that the modified design methods have the potential to be utilized for stiffened CFDST columns.

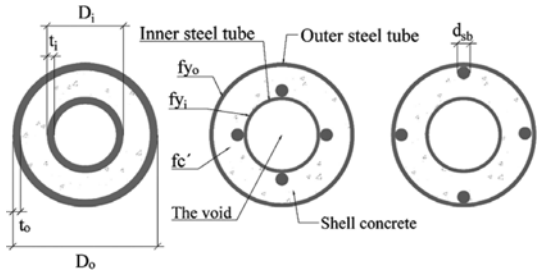

Fig. 1. CFDST Cross-section Details

2. Experimental Work

2.1 General

Two ordinary CFST specimens and two unstiffened CFDST columns were fabricated without WRBs are considered as a reference. Moreover, twelve-CFDST column specimens have been fabricated with WRBs. The specimens' geometry is observed in Fig. 2. Likewise, an overview of the parameters that were used in the current study and the rest of the details are listed in Table 1.

The labelling of the specimens included the numbers 1 and 2, where 1 refers to thin thicknesses of both the inner and outer tubes, whereas 2 refers to thick thicknesses of both tubes. The

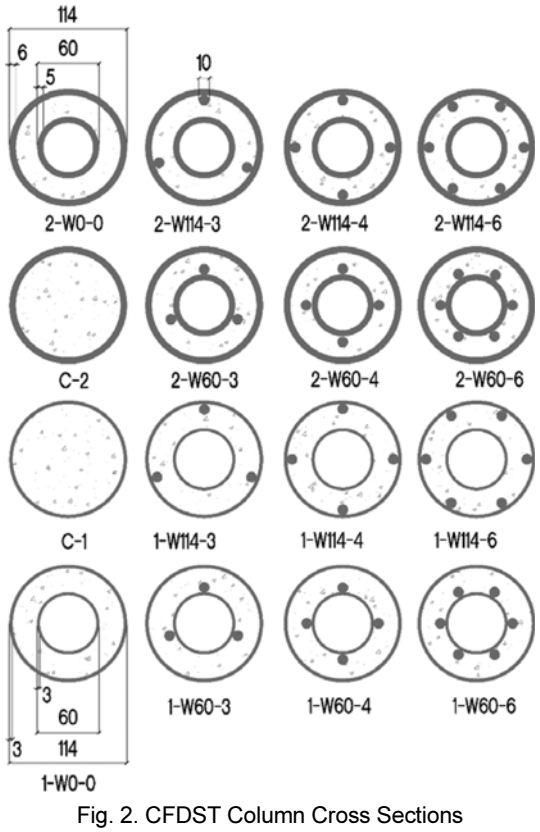

Fig. 2. CFDST Column Cross Sections

Table 1. Details of the Specimens

Column (ID)	L/Do	Do/t	Inner tube			Outer tube		
			D (mm)	t (mm)	f_y (Mpa)	D (mm)	t (mm)	f_y (Mpa)
Thin-thin specimens								
C-1	3.0	41.86	N/A	N/A	N/A	114.3	2.73	285
1-W0-0	3.0	41.86	60.3	2.56	380	114.3	2.73	285
1-W60-3	3.0	41.86	60.3	2.56	380	114.3	2.73	285
1-W114-3	3.0	41.86	60.3	2.56	380	114.3	2.73	285
1-W60-4	3.0	41.86	60.3	2.56	380	114.3	2.73	285
1-W114-4	3.0	41.86	60.3	2.56	380	114.3	2.73	285
1-W60-6	3.0	41.86	60.3	2.56	380	114.3	2.73	285
1-W114-6	3.0	41.86	60.3	2.56	380	114.3	2.73	285
Thick-thick specimens								
C-2	3.0	19.53	N/A	N/A	N/A	114.3	5.85	455
2-W0-0	3.0	19.53	60.3	4.71	435	114.3	5.85	455
2-W60-3	3.0	19.53	60.3	4.71	435	114.3	5.85	455
2-W114-3	3.0	19.53	60.3	4.71	435	114.3	5.85	455
2-W60-4	3.0	19.53	60.3	4.71	435	114.3	5.85	455
2-W114-4	3.0	19.53	60.3	4.71	435	114.3	5.85	455
2-W60-6	3.0	19.53	60.3	4.71	435	114.3	5.85	455
2-W114-6	3.0	19.53	60.3	4.71	435	114.3	5.85	455

labelling system includes the thickness of both tubes, position of WRBs, and the number of the WRBs, respectively. Furthermore, W60 denotes that reinforcing bars embedded with an inner steel tube, while, W114 represents the reinforcing bars embedded with an outer steel tube. For example, the label 1-W60-3 defines the CFDST column, where the number 1 refers to the specimen consists of a thin outer tube and a thin inner tube (thin-thin), W60 shows that the reinforcing bars were welded on the external surface of the inner steel tube, finally the number 3 represents the number of the welded reinforcing bars. On the other hand, the label 2-W0-0 defines the CFDST column, where the number 2 refers to the specimen consists of a thick outer tube and a thick inner tube (thick-thick), and no WRB embedded in this specimen. Besides, the character "C" represents CFST columns and considered as a reference. As an example, C-2 means CFST specimen with a thick outer steel tube, whereas C-1 means CFST specimen with a thin outer steel tube, as illustrated in Fig. 2.

2.2 Materials Properties

All of the steel tubes in the present study are cold-formed tubes which were produced according to EN 10219-1 (CEN, 2006). Two coupon specimens were cut from each tube to measure the actual yield strength of steel tubes (f_y) by coupon test according to (ASTM, 2015b), Fig. 3. ϕ10 mm diameter of deformed steel reinforcing bars was used with a yield strength of 430 MPa (ASTM, 2015a). One concrete class was produced. The concrete mix was prepared with the objective of obtaining normal self-compacted concrete class (C42 MPa). Four 100 × 200 mm cylinder moulds were cast with concrete to obtain the actual compressive strength (f_c). After completing the curing process, concrete samples were tested according to ASTM (2003).

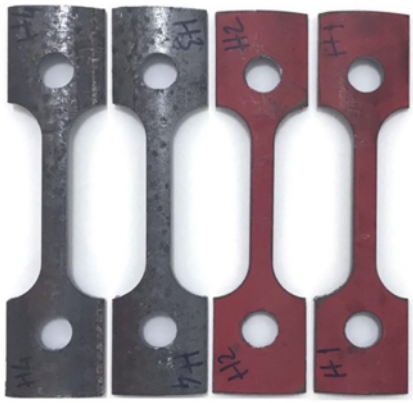

Fig. 3. Tensile Coupon Specimens

2.3 Test Setup and Fabrication

The dimensions of the steel tubes were selected to achieve an L/D ratio of 3.0. The overall behaviours of the small-scale units were quite similar to the full-scale specimen during testing (Zhu *et al.*, 2017). According to an L/D ratio and considering a further machining process, all hollow steel tubes were cut to lengths slightly greater than 343 mm. The machining process reduced both the steel tubes and WRBs to a final exact length of 343 mm (Ronald, 2010).

The diameters of the outer tubes of 114.3 mm with two thicknesses, where 5.85 mm for thickest outer diameters and 2.73 mm for thinnest outer diameters, whereas, the inner steel tubes have a diameter of 60.3 mm with two different thicknesses 4.71 mm and 2.56 mm. The diameters of reinforcing bars of 10 mm were used with a different number for each specimen (6, 4 and 3). The difference of specimen properties was selected to discover the influence of WRBs on the performance of CFDST columns.

All tests were completed with a universal testing machine with a capacity of 3,000 kN. Moreover, two LVDTs were located at two points in order to measure the shortening. The average values of the two LVDTs were used to draw the compression load-end shortening curves.

3. Results

The curves of compressive loading versus end shortening were offered during the tests and plotted for each specimen in Figs. 4, 5, 6, 7, 8, 9, 10 and 11. Furthermore, in Table 2, the ultimate axial load capacities were achieved in the tests for each column are listed.

3.1 Compression Loading versus End Shortening Curves

3.1.1 Specimens with Thin Steel Tubes

The reference specimen with thin tubes (thin-thin) and the CFDST specimen without WRBs (C-1, 1-W0-0) are presented in Fig. 4. Viewing the curves, it is interesting to observe that the 1-W0-0 specimen exhibits a greater performance over the reference specimen C-1 and behaves in a different manner. Furthermore, 1-W0-0 reached a compression capacity of 758.61 kN, which exceeds the value measured for the corresponding reference specimen C-1, when the C-1 specimen achieved 726.34 kN. At the compression capacity level, the C-1 specimen has an end shortening value of 3.41 mm. Besides, 1-W0-0 specimen behaves in a more ductile manner and has an end shortening value of 9.07 mm at the level of compression capacity. This fact explains that the increase in the nominal steel ratio helps to increase the ductility (Han *et al.*, 2009). Moreover, it can be explained that they have different initial stiffness values, this difference can be attributed to substituting concrete by an inner steel tube.

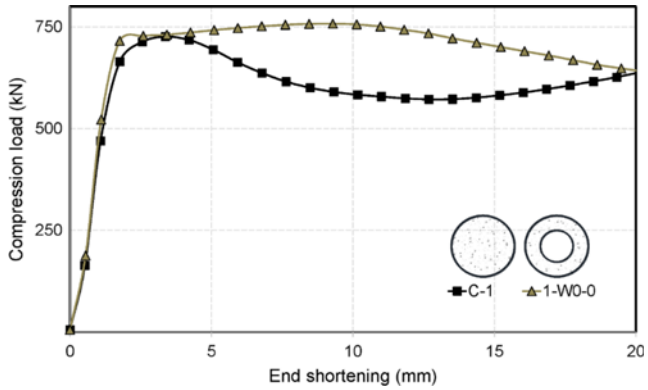

Fig. 4. Compression Load vs. End Shortening Curves for C-1 and 1-W0-0

Table 2. Experimental N_{exp}, CSCR and SI Results

Column (ID)	N_{exp} (kN)	CSCR	SI
Thinner-thinner			
C-1	726.34	1.00	1.19
1-W0-0	758.61	1.04	1.11
1-W60-3	862.48	1.19	1.10
1-W114-3	861.77	1.18	1.10
1-W60-4	907.88	1.25	1.11
1-W114-4	880.25	1.21	1.08
1-W60-6	999.49	1.38	1.13
1-W114-6	975.55	1.34	1.10
Thicker-thicker			
C-2	1,465.76	1.00	1.22
2-W0-0	1,622.25	1.11	1.11
2-W60-3	1,812.27	1.24	1.12
2-W114-3	1,745.14	1.19	1.16
2-W60-4	1,835.22	1.25	1.12
2-W114-4	1,789.22	1.22	1.15
2-W60-6	1,916.75	1.30	1.11
2-W114-6	1,850.37	1.26	1.15

Moreover, as listed in Table 2, the compression capacity of the specimens 1-W60-3, 1-W60-4 and 1-W60-6 achieved 862.48, 907.88 and 999.49 kN, respectively, whereas, the compression capacities of the specimens 1-W114-3, 1-W114-4 and 1-W114-6 achieved 861.77, 880.25 and 975.55 kN, respectively. It means that the compression capacity of the specimens was increasing as the number of WRBs increased. In addition, the specimens that have thin tubes with WRBs on the external surface of inner steel tube have slightly greater compression capacities compared to

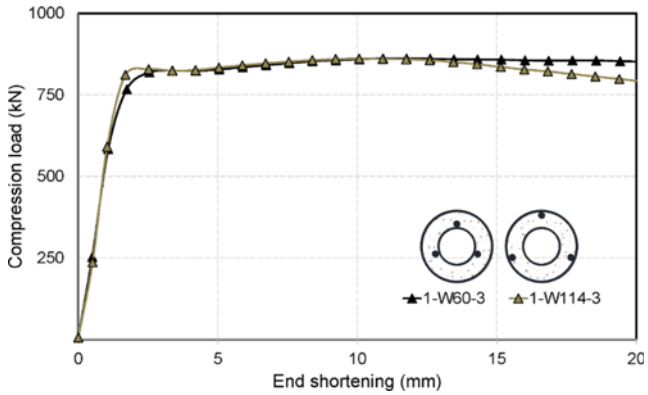

Fig. 5. Compression Load vs. End Shortening Curves for 1-W60-3 and 1-W114-3

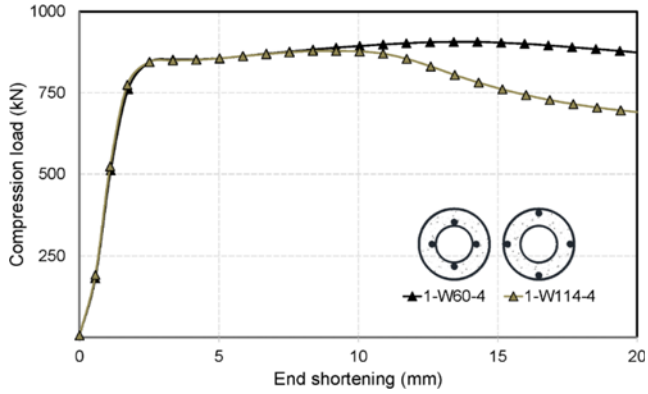

Fig. 6. Compression Load vs. End Shortening Curves for 1-W60-4 and 1-W114-4

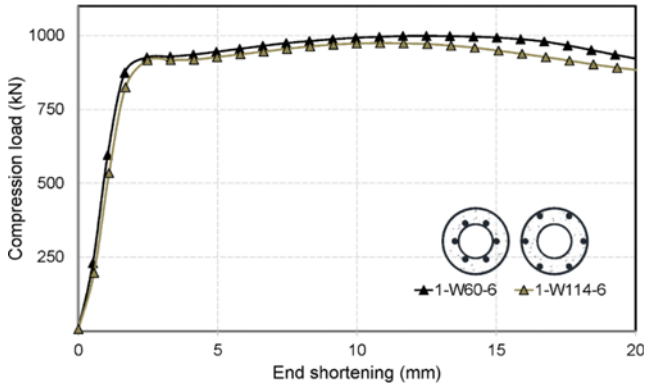

Fig. 7. Compression Load vs. End Shortening Curves for 1-W60-6 and 1-W114-6

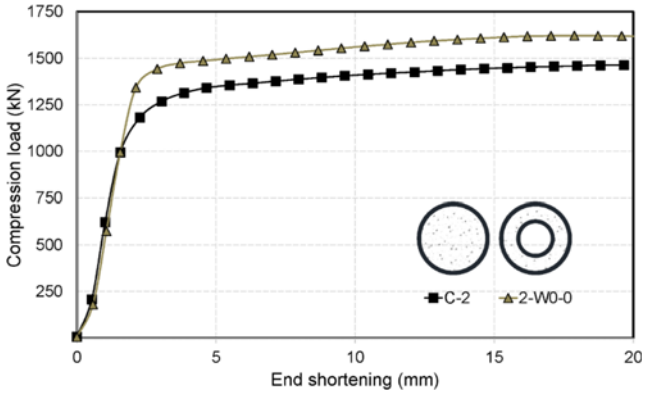

Fig. 8. Compression Load vs. End Shortening Curves for C-2 and 2-W0-0

the specimens that have WRBs on the internal surface of outer steel tubes, Figs. 5, 6 and 7.

At the compression capacity level, 1-W60-3 specimen has an end shortening value of 11.64 mm, whilst, 1-W114-3 specimen behaves in a less ductile manner and has an end shortening value of 10.16 mm. The specimens 1-W60-3 and 1-W114-3 behave in a similar manner, Fig. 5. On the other hand, the curves of the remaining specimens with thin tubes (thin-thin), 1-W60-4, 1-W114-4, 1-W60-6 and 1-W114-6 are presented in Fig. 6 and Fig. 7. The 1-W60-4 specimen has an end shortening value of 14.19 mm at the compression capacity level, whilst, 1-W114-4 specimen behaves in a less ductile manner and has an end shortening value of 9.07 mm. However, the compression capacity level of 1-W60-6 specimen has an end shortening value of 12.91 mm, whereas, 1-W114-6 specimen behaves in a less ductile manner and has an end shortening value of 10.92 mm at the level of compression capacity.

In terms of stiffness, it can be deduced that the specimens with thin tubes have a slight difference of initial stiffness values, this difference could be attributed to the different numbers and patterns of the WRBs. Interestingly, it was observed that all columns with WRBs on the external surface of inner steel tubes (1-W60-3, 1-W60-4, 1-W60-6) had slightly more ductile behaviour compared to those of the other pattern counterparts, (1-W114-3, 1-W114-4, 1-W114-6).

3.1.2 Specimens with Thick Steel Tubes

As shown in Fig. 8, the reference specimen (C2) and the unstiffened CFDST specimen (2-W0-0) behave similarly. Furthermore, the 2-W0-0 specimen exhibits a greater performance over the reference specimen C-2, which the 2-W0-0 specimen reached a compression capacity of 1,622 kN. On the other hand, the corresponding reference specimen C-2 achieved 1,465 kN, Table 2.

The compression capacities of the specimens 2-W60-3, 2-W60-4 and 2-W60-6 reached 1,812.27, 1,835.22 and 1,916.75 kN, respectively. However, the compression capacities of the specimens 2-W114-3, 2-W114-4 and 2-W114-6 achieved 1,745.14, 1,789.22 and 1,850.37 kN, respectively. It means that the compression capacities of these specimens were increasing as

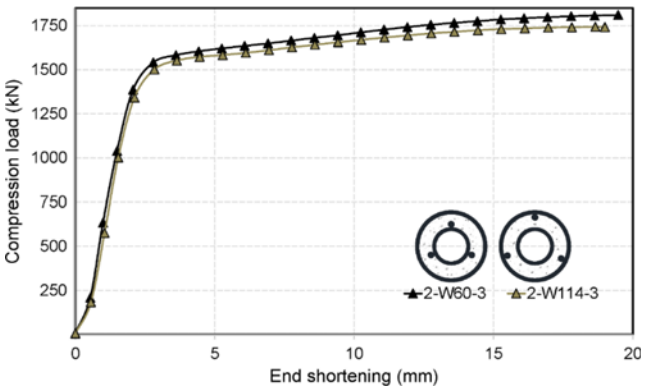

Fig. 9. Compression Load vs. End Shortening Curves for 2-W60-3 and 2-W114-3

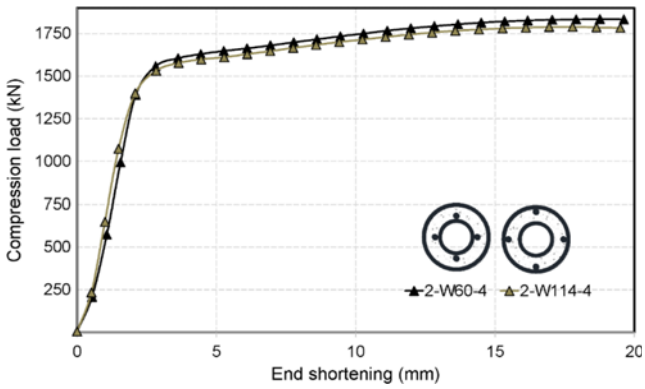

Fig. 10. Compression Load vs. End Shortening Curves for 2-W60-4 and 2-W114-4

the number of WRBs increased. Likewise, the specimens that have thick tubes with WRBs on the external surface of inner steel tubes have greater compression capacities compared to those of the other pattern counterparts, Figs. 9, 10 and 11.

Viewing of curves, Figs.9, 10 and 11, the specimens 2-W60-3, 2-W60-4 and 2-W60-6 have a higher slope than the 2-W114-3, 2-W114-4 and 2-W114-6, respectively. On the other hand, at the compression capacities level, 2-W60-3, 2-W60-4 and 2-W60-6 specimens have an end shortening value of 19.89 mm, 18.84 mm

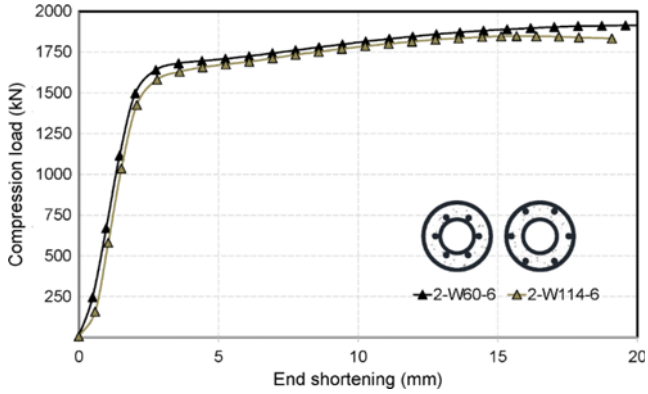

Fig. 11. Compression Load vs. End Shortening Curves for 2-W60-6 and 2-W114-6

and 20.43 mm, respectively. However, 2-W114-3, 2-W114-4 and 2-W114-6 specimens have an end shortening value of 18.09 mm, 17.8 mm and 15.64 mm, respectively. It is important to mention that the specimens that have WRBs with inner steel tubes have slightly greater initial stiffness compared to the specimens that have WRBs with outer steel tubes counterparts, Figs. 9, 10 and 11.

3.2 Concrete-Steel Contribution Ratio (CSCR)

The contribution of the tubes in double skin columns is elaborated in this study by focusing on the impact of the WRBs and the steel tubes thicknesses on the compression capacities. Besides, the abbreviation CSCR means concrete-steel contribution ratio, which was utilized by Ibañez *et al.* (2017). CSCR is a ratio between $N_{u,CFDST}$ to $N_{u,CFST}$, where $N_{u,CFDST}$ is the ultimate load achieved for the CFDST specimen (stiffened or unstiffened), and $N_{u,CFST}$ is the ultimate load achieved for the ordinary CFST specimen counterpart as shown in Eq. (1). This ratio can assess the enhancement of the mechanical response of a double skin column based on the response of a CFST column counterpart as follows:

$$CSCR = \frac{N_{u,CFDST}}{N_{u,CFST}} \tag{1}$$

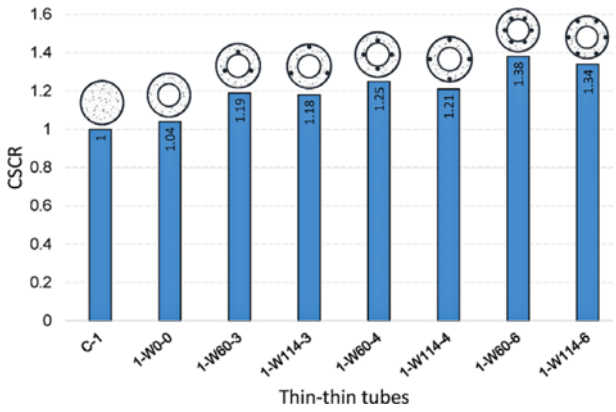

Fig. 12. Concrete-steel Contribution Ratio for (Thin-thin Tubes) Specimens

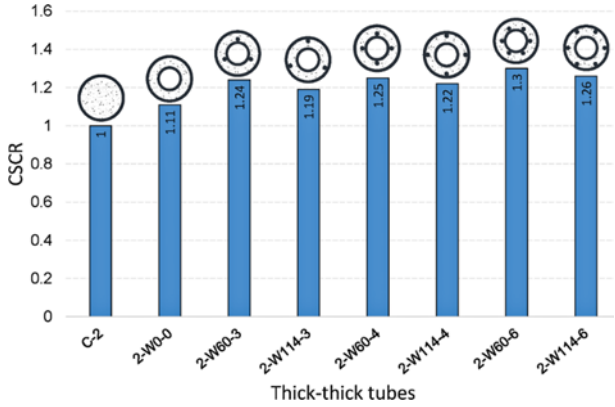

Fig. 13. Concrete-steel Contribution Ratio for (Thick-thick Tubes) Specimens

Figure 12 illustrates that the CSCR was more than unity in the specimens with thin-thin tubes, where the specimens 1-W60-3, 1-W114-3, 1-W60-4, 1-W114-4, 1-W60-6 and 1-W114-6 have CSCRs of 1.18, 1.18, 1.24, 1.21, 1.37 and 1.34 respectively. On the other hand, the specimens 2-W60-3, 2-W60-4, 2-W60-6, 2-W114-3, 2-W114-4 and 2-W114-6 have CSCR of 1.24, 1.25, 1.30 1.19, 1.22 and 1.26, respectively. Fig. 13 indicates that the CSCR of these specimens were increasing as the number of WRBs increased. Correspondingly, these patterns of WRB affect positively on the mechanical response of the CFDST specimens. Moreover, it is interesting here to observe that the CSCR of the stiffened CFDST specimens that have WRB with inner steel tube are higher than the CSCR of specimens that have the other pattern counterparts.

On the other hand, the CSCR of the unstiffened CFDST specimens (without WRB) 1-W0-0 and 2-W0-0 are more than unity, as listed in Table 2. It means that the inner tube affects positively on the compression capacity of the double skin columns and did enhance the behaviour of the ordinary CFST columns counterparts.

3.3 Compressive Strength Index (SI)

The strength index of the CFDST column includes four elements: the shell concrete, the inner tube, the outer tube, and WRBs as defined in Eq. (2) shown below:

$$SI = \frac{N_{exp}}{A_{so}f_{yo} + 0.85A_cf_c + A_{si}f_{yi} + A_{sb}f_{ysb}} \tag{2}$$

where N_{exp} is the calculated ultimate strength of specimen and A_{so}, A_c, A_{si} and A_{sb} are the areas of the outer tube, sandwiched concrete, inner tube, and WRB, respectively. Eq. (2) is used for specimens C-1 and C-2 after ignoring both terms of $A_{si}f_{si}$ and $A_{sb}f_{ysb}$ for these specimens. Likewise, it is used for 1-W0-0 and 2-W0-0 also after ignoring the terms of $A_{sb}f_{ysb}$ for these specimens. As listed in Table 2, the SI for all columns are more than unity. It means that the confinement of concrete in the specimens is clear, leading to apparent concrete strength improvement (Wang *et al.*, 2017). It can indicate that the confinement performance of

the specimen is increasing as the number of WRBs increase. Furthermore, it seems that the specimens with WRBs on the external surface of inner steel tubes have slightly greater SI compared to SI of the specimens that have WRBs with outer steel tubes counterparts.

4. Failure Modes

In order to differentiate the performance of CFDST and the extent of the WRBs contribution of these columns, it is essential to observe the shape of the tube's failure. The specimens C-1 and 1-W0-0 were used for comparison purposes. The failure mode of the specimen 1-W0-0 is different when compared to the failure modes of the remaining specimens as shown in Figs. 14 and 15. It has harsh and intense local failure mode, especially at the inner steel tube. This level of inward and outward buckling occurred due to the weakness of the inner support with the thin-thin tubes against expansion in the shell concrete, as shown in Fig. 14(b). It is crucial to note that the specimens with thin tubes showed evidence of shear cracks in concrete.

On the other hand, Figs. 14 and 15 show that increasing the number of the WRBs eliminate the harmful effect of the local bulking. Furthermore, the specimens 1-W60-4 and 1-W60-6 have significant resistance against inward and outward distortions, whereas, the specimens 1-W114-4 and 1-W114-6 exhibited significantly inward and outward distortions, Fig. 15. This means that the specimens with WRBs on the thin inner tubes have a promising performance and achieved smaller inward and outward distortions than the thin-thin specimens with WRBs on the outer tubes. Generally, it could be observed that the specimens with thin tubes exhibit significantly more lateral deformations compared to the specimens with thick-thick tubes. It indicates that the thin tubes cannot provide an appropriate composite action which allows the concrete and steel tube to serve together properly. It is important in composite structural members to satisfy this harmony.

It can be observed in Figs. 16 and 17, the thick steel tubes have a very promising performance as these configurations (thick-thick) attained very small inward and outward distortions. It indicates that a thick inner tube with a thick outer tube serve the cross-sectional capacity efficiently. Hence, this configuration can

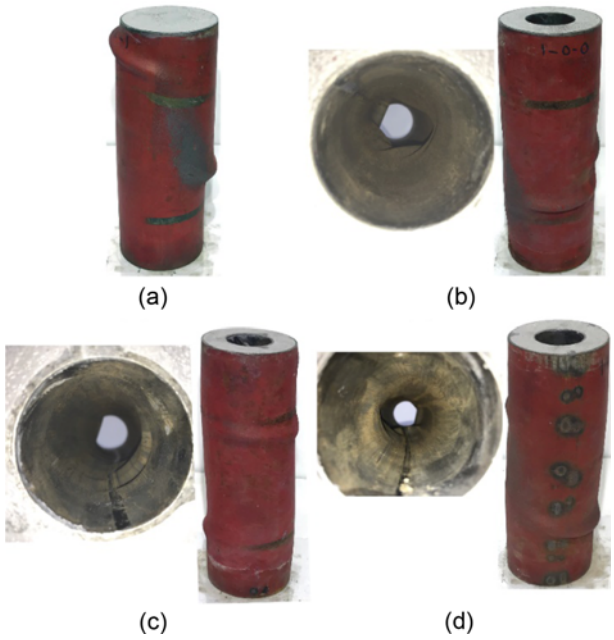

Fig. 14. Failure Modes of: (a) C-1 Specimen, (b) 1-W0-0 Specimen, (c) 1-W60-3 Specimen, (d) 1-W114-3 Specimen

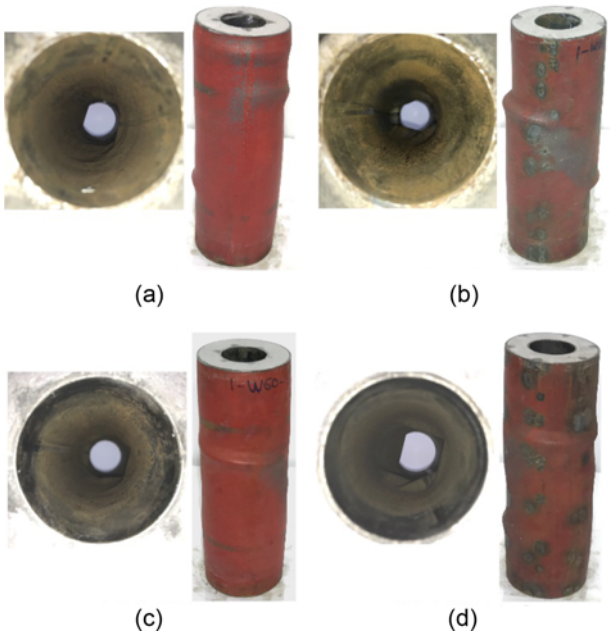

Fig. 15. Failure Modes of: (a) 1-W60-4 Specimen, (b) 1-W114-4 Specimen, (c) 1-W60-6 Specimen, (d) 1-W114-6 Specimen

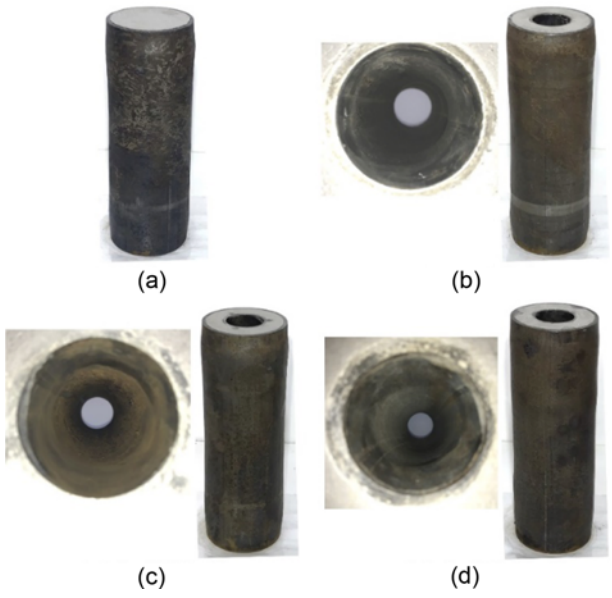

Fig. 16. Failure Modes of: (a) C-2 Specimen, (b) 2-W0-0 Specimen, (c) 2-W60-3 Specimen, (d) 2-W114-3 Specimen

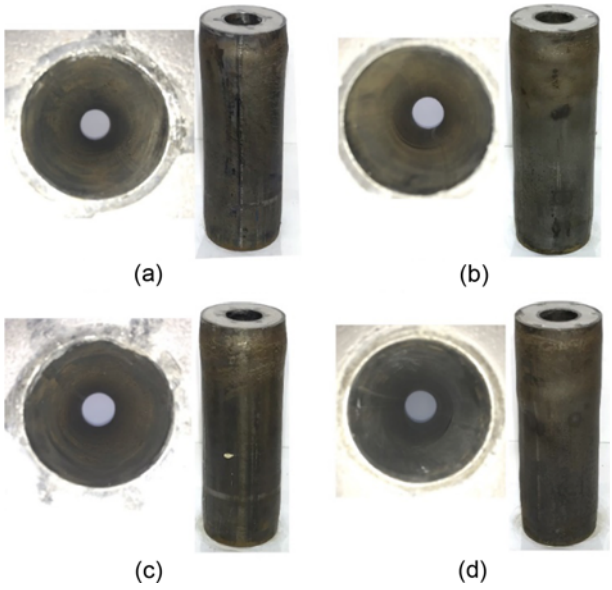

Fig. 17. Failure Modes of: (a) 2-W60-4 Specimen, (b) 2-W114-4 Specimen, (c) 2-W60-6 Specimen, (d) 2-W114-6 Specimen

develop good "composite action" with the shell concrete. In addition, the thick tubes governed the compression behaviour of the columns and did not allow the specimens to exhibit shear failure modes.

5. Comparisons with Design Methods of CFDST Columns

The aim of this section is to estimate the compressive strengths of the stiffened double skin columns by using the design methods that were proposed by several investigators. Generally, the design procedures of unstiffened CFDST column were extended for stiffened CFDST column by changing certain parameters, such as Han *et al.* (2009), and Yu *et al.* (2013) methods which were used in this study. In addition, the design process of columns that are detailed in the Eurocode 4 (CEN, 2004) and AISC-360 (AISC, 2016) standards were also developed to predict the cross-section capacities of circular stiffened CFDST columns.

5.1 AISC-360

The strength capacity (N_n) of the ordinary CFST column in Eq. (3) (AISC, 2016) was changed to apply for CFDST column by Sulthana and Jayachandran (2017), as given in Eq. (4). Furthermore, the authors proposed Eq. (5), where the strength generated by the WRBs added to Eq. (4):

$$P_n = f_{yo}A_{so} + C_2 f_c' A_c \tag{3}$$

$$P_n = f_{yo}A_{so} + A_i f_{yi} + C_2 f_c' A_c \tag{4}$$

$$P_{n,mod} = f_{yo}A_{so} + A_i f_{yi} + C_2 f_c' A_c + A_{sb} f_{ysb} \tag{5}$$

The C_2 factor takes 0.95 when the inner and outer steel tubes are circular, otherwise, it assumes 0.85. The elastic buckling load (P_{cr}) and the strength capacity (P_{AISC}) of a column are displayed in Eqs. (7) and (6) respectively:

$$P_{AISC,mod} = \begin{cases} P_n[0.658^{P_n/P_{cr}}] & : \dfrac{P_n}{P_{cr}} \le 2.25 \\ 0.877 P_{cr} & : \dfrac{P_n}{P} > 2.25 \end{cases} \tag{6}$$

$$P_{cr} = \frac{\pi^2 EI_{eff}}{L^2} \tag{7}$$

where EI_{eff} is the effective flexural rigidity of the cross-section, as given in Eqs. (8) and (9):

$$EI_{eff} = E_{so}I_{so} + E_{si}I_{si} + C_3 E_c I_c \tag{8}$$

$$C_3 = 0.6 + 2\left(\frac{A_{so}+A_{si}}{A_{so}+A_{si}+A_c}\right) \le 0.9 \tag{9}$$

5.2 EC4

The strength of cross-section (N_n) of ordinary CFST column according to CEN (2004) is given in Eq. (10). Based on CEN (2004), Pagoulatou *et al.* (2014) suggested the compressive strength equation for CFDST columns with inner and outer tubes, as given in Eq. (11). Moreover, the strength capacity of WRBs added to Eq. (11) as shown in Eq. (12):

$$N_u = \eta_s A_s f_y + Acfc\left(1 + \eta_c \frac{t f_y}{D f_c}\right); \text{ for } CFST \tag{10}$$

$$N_u = \eta_{so}(A_{so}f_{yo} + A_{si}f_{yi}) + Acfc\left(1 + \eta_c \frac{t_o f_{yo}}{D_o f_c}\right) : \text{ for } CFDST \tag{11}$$

$$N_{u,mod} = \eta_{so}(A_{so}f_{yo} + A_{si}f_{yi} + A_{sb}f_{ysb}) + Acfc\left(1 + \eta_c \frac{t_o f_{yo}}{D_o f_c}\right);$$

for CFDST with welded reinforcing bars (12)

The squash load of the column reduces by the stability reduction factor χ, which depends on the slenderness ratio (λ), as given in Eq. (15). The calculation of λ is assumed in Eq. (13), where N_{cr} is the elastic buckling load of the column and N_u is the cross-section capacity. Furthermore, the effective flexural rigidity (EI_{eff}) is specified in Eq. (14):

$$\lambda = \sqrt{\frac{N_u}{N_{cr}}} \tag{13}$$

$$EI_{eff} = E_{so}I_{so} + E_{si}I_{si} + 0.6E_c I_c \tag{14}$$

$$N_{u,EC4,mod} = \chi(A_{so}f_{yo} + A_{si}f_{yi} + Acfc + A_{sb}f_{ysb}) \tag{15}$$

$$\chi = \frac{1}{\phi + \sqrt{\phi^2 - \lambda^2}} \tag{16}$$

$$\phi = 0.5(1 + \alpha(\lambda - 0.2) + \lambda^2) \tag{17}$$

5.3 Design Strength by Han

Han *et al.* (2009) proposed a new formulation to predict the cross-section capacity of unstiffened CFDST specimen, where the effect of the confinement is considered in the shell concrete strength. The maximum squash load of the unstiffened CFDST column measured as follows:

$$N_{u,Han} = N_{i,u} + N_{osc,u} \tag{18}$$

In the present study, the cross-section capacity of the WRBs is linearly added to the squash load equation of CFDST column as follows:

$$N_{u,Han,mod} = N_{i,u} + N_{sb} + N_{osc,u} \quad (19)$$

where, $N_{i,u} = A_{si} f_{syi}$; $N_{sb} = A_{sb} fy_{sb}$; $N_{osc,u} = f_{scy} A_{sco}$; and $k_1 = 1$ when the tube thickness is less than 16 mm;

$$f_{scy} = k_1 C_1 \chi^2 f_{syo} + C_2 (1.14 + 1.02\xi_o) f_{ck} \quad (20)$$

where, $\chi = \frac{d}{D-2t_o}$; $\alpha = \frac{A_{so}}{A_c}$; $\alpha_n = \frac{A_{so}}{A_{ce}}$; $A_{ce} = \frac{\pi}{4}(d-2t_{so})^2$;

$C_1 = \frac{\alpha}{(1+\alpha)}$; $\xi = \alpha_n \frac{f_{syo}}{f_{ck}}$; $C_2 = \frac{(1+\alpha_n)}{(1+\alpha)}$; $A_{sco} = A_{so} + A_c$; and

$f_{ck} = \frac{f_c'}{1.5}$

The χ is hollowness ratio and ξ is a confinement ratio factor. Besides, $C1$ and $C2$ are factors based on component area (area of concrete and steel).

5.4 Design Strength by Yu

A strength capacity of the CFST column was suggested by Yu *et al.* (2013), as follows:

$$N_{u,Yu} = (1 + 0.5(\xi/1 + \xi)\Omega)(f_{sy} A_s + f_{ck} A_c) \quad (21)$$

where, $\zeta = (\alpha . f_{sy}/f_{ck})$, $\alpha = (A_s/A_c)$, Ω is a solid proportion, as $\Omega = A_c/(A_c + A_k)$, A_s is an outer steel tube area, A_c is a shell concrete area, and A_k is a hollow part area. The strength capacity ($N_{u,Yu,cFDST}$) of the unstiffened CFDST column was modified by Hassanein and Kharoob (2014), where the squash load of inner steel tube added to Eq. (21), hence, the equation of the unstiffened CFDST columns is considered as follows:

$$N_{u,Yu,CFDST} = (1 + 0.5(\xi/1 + \xi)\Omega)(f_{syo} A_{so} + f_{ck} A_c) + N_{i,u}; \quad (N_{i,u} = f_{syi} A_{si}) \quad (22)$$

The strength generated by the welded reinforcing bars (N_{sb}) added to Eq. (22) to obtain the squash load of the stiffened CFDST column as follows:

$$N_{u,Yu,mod} = (1 + 0.5(\xi/1 + \xi)\Omega)(f_{syo} A_{so} + f_{ck} A_c) + N_{i,u} + N_{sb} \quad (23)$$

where $N_{sb} = f_{sby} A_{sb}$, A_{si} is an area of the inner tube, A_{so} is an area of the outer tube, f_{syi} is yield stress of the inner tube, f_{syo} is yield stress of the outer tube and f_{sby} is yield stress of the reinforcing bars.

5.5 Results of Strength Predictions

The calculated strength predictions using the above-mentioned modified methods ($N_{EC4,mod}$, $N_{AISC,mod}$, $N_{Han,mod}$, and $N_{Yu.mod}$). It can be shown in Table 3, the $N_{EC4.mod}/N_{exp}$ ratios are less than one with some exceptions. However, the mean value and the standard deviation of $N_{EC4.mod}/N_{exp}$ ratios are 0.97 and 0.03, respectively. The $N_{AISC.mod}/N_{exp}$ ratios are also lower than one, where the mean value and the standard deviation of $N_{AISC.mod}/N_{exp}$ ratios are 0.90 and 0.03, respectively. This means that the EC4$_{mod}$ method offers the best and more accurate predictions of the strength capacity for stiffened CFDST columns compared to AISC$_{mod}$ method, Fig. 18.

Table 3. Comparison of Strength Predictions with Test Results

Specimen	N_{exp}	$N_{EC4.mod}/N_{exp}$	$N_{AISC.mod}/N_{exp}$	$N_{Han.mod}/N_{exp}$	$N_{Yu.mod}/N_{exp}$
Thin-thin					
C-1	726.34	0.89	0.89	0.88	0.93
1-W0-0	758.61	1.02	0.93	0.93	0.96
1-W60-3	862.48	0.99	0.93	0.93	0.96
1-W114-3	861.77	0.99	0.93	0.93	0.96
1-W60-4	907.88	0.97	0.92	0.92	0.95
1-W114-4	880.25	1.00	0.95	0.95	0.98
1-W60-6	999.49	0.93	0.91	0.91	0.93
1-W114-6	975.55	0.95	0.93	0.93	0.95
Thick-thick					
C-2	1,465.76	0.94	0.84	1.01	1.09
2-W0-0	1,622.25	1.01	0.91	1.01	1.06
2-W60-3	1,812.27	0.95	0.87	0.96	1.00
2-W114-3	1,745.14	0.99	0.90	1.00	1.04
2-W60-4	1,835.22	0.95	0.87	0.97	1.01
2-W114-4	1,789.22	0.98	0.90	0.99	1.03
2-W60-6	1,916.75	0.94	0.87	0.96	1.00
2-W114-6	1,850.37	0.97	0.90	1.00	1.04
Mean		0.97	0.90	0.95	0.99
Standard deviations		0.03	0.03	0.04	0.05

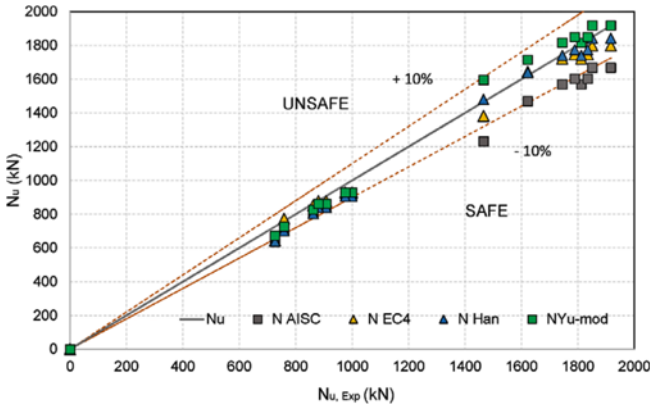

Fig. 18. Comparison of Experimental Ultimate Loads and Design Methods Prediction

On the other hand, the $N_{Han.mod}/N_{exp}$ ratios are lower than one with some exceptions, where the mean value and the standard deviation of $N_{Han.mod}/N_{exp}$ ratios are 0.95 and 0.04, respectively. The mean value and the standard deviation of $N_{Yu.mod}/N_{exp}$ ratios are 0.99 and 0.05, respectively. It means that the Han$_{mod}$ method offers safe prediction of the strength capacity of the stiffened CFDST columns compared to Yu$_{mod}$ method. It means that the estimates of Yu$_{mod}$ method are slightly unconservative related to thick tubes (thick-thick) combinations in these stiffened CFDST columns.

6. Conclusions

The current study presented an experimental work on the CFDST column stiffened by Welded Reinforcing Bars (WRBs) under compressive loading. A series of tests were conducted on sixteen CFDST specimens. Two different D/t ratios and different patterns of WRBs were used as parameters to enable a better understanding of the performance of the stiffened CFDST column. For that purpose, compressive loading vs. end shortening curves, failure modes, strength index and concrete-steel contribution ratio were analysed. Finally, the design methods that were used in previous studies have been developed for comparison with experimental results. Based on the results, the subsequent conclusions can be drawn within the scope of this study:

1. The compression loading vs. end shortening curves of CFDSTs revealed that the strength capacity, ductility, stiffness, and toughness were increasing as the number of WRBs and/or thickness of the steel tubes increased. Likewise, the buckling of columns can be effectively postponed by increasing the number of WRBs on the steel tubes.
2. The specimens with WRBs on the external surface of inner tubes have a greater promising performance than the specimens that have WRBs on the internal surface of outer tubes, and achieved smaller inward and outward distortions. Furthermore, the installation of the first pattern (WRBs with inner tubes) is easier than the other pattern counterpart even with the steel tubes that have a small diameter. Accordingly, to provide the desired level of performance of CFDST columns, it would be preferable to weld reinforcing bars on the external surface of the inner tubes.
3. Obviously, the contribution of WRBs is less significant with the thick tubes (thick-thick) in CFDST column, whereas, the WRBs are more significant with thin tubes.
4. In terms of CSCRs, all specimens can gain the compression capacity more than the thin-walled CFST columns counterpart with less weight. In addition, the WRBs with inner steel tubes affect positively on the mechanical response of CFDST columns, which confirms their effectiveness slightly higher than those that have WRBs with outer steel tubes. Additionally, SI of the columns increased as the number of WRBs increased, consequently, it can indicate that the confinement performance of the specimen is increasing as the number of WRBs increases.
5. In terms of failure modes, the thick-thick configurations have a very promising performance and attained very small inward and outward distortions. Hence, the thick tubes can develop good ‘‘composite action’’ with the shell concrete. Moreover, the thick tubes governed the compression behaviour of the columns and did not allow the specimens to exhibit shear failure modes.
6. The modified methods of EC4 and Han offer better and more accurate predictions of the strength capacity for the stiffened CFDST columns. As shown, the predictions provided by using these design methods are always on the safe side. These modified formulas will be very useful to the structural designers for a prescribed strength capacity of CFDST columns.
7. The modified AISC method gives very conservative predictions of the stiffened CFDST columns, which were about 10% lower than those of the experiments.
8. The modified Yu method offered unconservative predictions of the strength capacity for stiffened CFDST columns with some exceptions related to the thin-thin steel tubes combinations, and thereby it does not satisfy the safety requirements.

Although this paper focuses on the experimental and theoretical study of stiffened CFDST columns under axial compression, additional research is needed to investigate the behaviour of stiffened CFDST columns by using Finite element methods in order to investigate if the FEM analysis is capable of predicting the behaviour of stiffened CFDST columns or not.

Acknowledgements

The authors express their sincere gratitude to BASF/Turkey-Gaziantep for supplying the concrete admixtures that were used in this study.

References

Abbas, H., Al-Salloum, Y., Alsayed, S., Alhaddad, M., and Iqbal, R. (2017). “Post-heating response of concrete-filled circular steel columns.” *KSCE Journal of Civil Engineering*, Vol. 21, No. 4, pp. 1367-1378, DOI:10.1007/s12205-016-0852-3.

AISC (2016). *Specification for structural steel buildings,* ANSI/AISC 360-16, American Institute of Steel Construction, Chicago, IL, USA.

Aslani, F., Uy, B., Hur, J., and Carino, P. (2017). “Behaviour and design of hollow and concrete-filled spiral welded steel tube columns subjected to axial compression.” *Journal of Constructional Steel Research*, Vol. 128, pp. 261-288, DOI: 10.1016/j.jcsr.2016.08. 023.

Aslani, F., Uy, B., Tao, Z., and Mashiri, F. (2015a). “Behaviour and design of composite columns incorporating compact high-strength steel plates.” *Journal of Constructional Steel Research*, Vol. 107, pp. 94-110, DOI: 10.1016/j.jcsr.2015.01.005.

Aslani, F., Uy, B., Tao, Z., and Mashiri, F. (2015b). “Predicting the axial load capacity of high-strength concrete filled steel tubular columns.” *Steel and Composite Structures*, Vol. 19, No. 4, pp. 967-993, DOI: 10.12989/scs.2015.19.4.967.

Aslani, F., Uy, B., Wang, Z., and Patel, V. (2016). “Confinement models for high strength short square and rectangular concrete-filled steel tubular columns.” *Steel and Composite Structures*, Vol. 22, No. 5, pp. 937-974, DOI: 10.12989/scs.2016.22.5.937.

ASTM (2003). *Standard test method for compressive strength of cylindrical concrete specimens*, C39/C39M-03, ASTM International, West Conshohocken, PA, USA, DOI: 10.1520/C0039_C0039M-03.

ASTM (2015a). *Standard specification for deformed and plain carbon-steel bars for concrete reinforcement*, A615/A615M, ASTM International, West Conshohocken, PA, USA, DOI: 10.1520/A0615_A0615M-18E01.

ASTM (2015b). *Standard test methods for tension testing of metallic materials-standard*, E8/E8M-16a, ASTM International, West Conshohocken, PA, USA, DOI: 10.1520/E0008_E0008M-16A.

CEN (2004). *Eurocode 4: Design of composite steel and concrete*

structures - Part 1-1: General rules and rules for buildings, BS EN 1994-1-1:2004, European Committee for Standardization, Brussel, Belgium.

CEN (2006). *Cold formed welded structural hollow sections of non-alloy and fine grain steels - Part 1: Technical delivery conditions*, BS EN 10219-1:2006, European Committee for Standardization, Brussel, Belgium.

Dabaon, M., El-Khoriby, S., El-Boghdadi, M., and Hassanein, M. F. (2009). "Confinement effect of stiffened and unstiffened concrete-filled stainless steel tubular stub columns." *Journal of Constructional Steel Research*, Vol. 65, Nos. 8-9, pp. 1846-1854, DOI: 10.1016/j.jcsr.2009.04.012.

Dong, C. and Ho, J. C. M. (2013). "Improving interface bonding of double-skinned CFST columns." *Magazine of Concrete Research*, Vol. 65, No. 20, pp. 1199-1211, DOI: 10.1680/macr.13.00041.

Ekmekyapar, T., Alwan, O. H., Hasan, H. G., Shehab, B. A., and AL-Eliwi, B. J. (2019). "Comparison of classical, double skin and double section CFST stub columns: Experiments and design formulations." *Journal of Constructional Steel Research*, Vol. 155, pp. 192-204, DOI: 10.1016/j.jcsr.2018.12.025.

Elchalakani, M., Hassanein, M., Karrech, A., and Yang, B. (2018). "Experimental investigation of rubberised concrete-filled double skin square tubular columns under axial compression." *Engineering Structures*, Vol. 171, pp. 730-746, DOI: 10.1016/j.engstruct. 2018. 05.123.

Elchalakani, M., Zhao, X.-L., and Grzebieta, R. (2002). "Tests on concrete filled double-skin (CHS outer and SHS inner) composite short columns under axial compression." *Thin-Walled Structures*, Vol. 40, No. 5, pp. 415-441, DOI: 10.1016/S0263-8231(02)00009-5.

Essopjee, Y. and Dundu, M. (2015). "Performance of concrete-filled double-skin circular tubes in compression." *Composite Structures*, Vol. 133, pp. 1276-1283, DOI: 10.1016/j.compstruct.2015. 08.033.

Fu, Z., Wang, Q., Wang, Y., and Ji, B. (2018). "Bending performance of lightweight aggregate concrete-filled steel tube composite beam." *KSCE Journal of Civil Engineering*, Vol. 22, No. 9, pp. 1-9, DOI: 10.1007/s12205-018-0660-z.

Ge, H. and Usami, T. (1992). "Strength of concrete-filled thin-walled steel box columns: Experiment." *Journal of Structural Engineering*, Vol. 118, No. 11, pp. 3036-3054, DOI: 10.1061/(ASCE)0733-9445(1992)118:11(3036).

Gopal, S. R. (2017). "An experimental study on FRC infilled steel tubular columns under eccentric loading." *KSCE Journal of Civil Engineering*, Vol. 21, No. 3, pp. 923-927, DOI: 10.1007/s12205-016-0851-4.

Han, L.-H., Huang, H., and Zhao, X.-L. (2009). "Analytical behaviour of Concrete-filled Double Skin Steel Tubular (CFDST) beam-columns under cyclic loading." *Thin-Walled Structures*, Vol. 47, No. 6, pp. 668-680, DOI: 10.1016/j.tws.2008.11.008.

Han, L.-H., Li, W., and Bjorhovde, R. (2014). "Developments and advanced applications of Concrete-filled Steel Tubular (CFST) structures: Members." *Journal of Constructional Steel Research*, Vol. 100, pp. 211-228, DOI: 10.1016/j.jcsr.2014.04.016.

Hassan, M. M., Mahmoud, A. A., and Serror, M. H. (2016). "Behavior of concrete-filled double skin steel tube beam-columns." *Steel and Composite Structures*, Vol. 22, No. 5, pp. 1141-1162, DOI: 10.12989/scs.2016.22.5.1141.

Hassanein, M. and Kharoob, O. (2014). "Compressive strength of circular concrete-filled double skin tubular short columns." *Thin-Walled Structures*, Vol. 77, pp. 165-173, DOI: 10.1016/j.tws.2013. 10.004.

Hui, L., Bo, W., and Li—yan, L. (1998). "Study on seismic properties of laminated column with high strength concrete containing steel tube." *Earthquake Engineer ing and Engineering Vibration*, Vol. 18, No. 1, pp. 45-52.

Ibañez, C., Romero, M. L., Espinos, A., Portolés, J., and Albero, V. (2017). "Ultra-high strength concrete on eccentrically loaded slender circular concrete-filled dual steel columns." *Structures*, Vol. 12, pp. 64-74, DOI: 10.1016/j.istruc.2017.07.005.

Kim, D.-W. and Shim, C.-S. (2016). "Experiments on flexural strength on composite modular bridge pier cap for CFT columns." *KSCE Journal of Civil Engineering*, Vol. 20, No. 6, pp. 2483-2491, DOI: 10.1007/s12205-015-1467-9.

Kwan, A., Dong, C., and Ho, J. (2016). "Axial and lateral stress–strain model for circular concrete-filled steel tubes with external steel confinement." *Engineering Structures*, Vol. 117, pp. 528-541, DOI: 10.1016/j.engstruct.2016.03.026.

Lai, M. and Ho, J. (2014). "Confinement effect of ring-confined concrete-filled-steel-tube columns under uni-axial load." *Engineering Structures*, Vol. 67, pp. 123-141, DOI: 10.1016/j.engstruct. 2014.02.013.

Lee, S.-H., Choi, Y.-H., Kim, Y.-H., and Choi, S.-M. (2012). "Structural performance of welded built-up square CFST stub columns." *Thin-Walled Structures*, Vol. 52, pp. 12-20, DOI: 10.1016/j.tws.2011. 09.003.

Lin, T., Huang, C., and Chen, S. (1993). "Concrete-filled tubular steel columns subjected to eccentric axial load." *J. Chin. Inst. Civil Hydraulic Eng*, Vol. 54, pp. 377-386.

Pagoulatou, M., Sheehan, T., Dai, X., and Lam, D. (2014). "Finite element analysis on the capacity of circular Concrete-filled Double-skin Steel Tubular (CFDST) stub columns." *Engineering Structures*, Vol. 72, pp. 102-112, DOI: 10.1016/j.engstruct.2014.04.039.

Park, T., Hwang, W.-S., Leon, R. T., and Hu, J. W. (2011). "Damage evaluation of composite-special moment frames with concrete-filled tube columns under strong seismic loads." *KSCE Journal of Civil Engineering*, Vol. 15, No. 8, pp. 1381-1394, DOI: 10.1007/s12205-011-1225-6.

Romero, M. L., Ibañez, C., Espinós, A., Portolés, J., and Hospitaler, A. (2017). "Influence of ultra-high strength concrete on circular concrete-filled dual steel columns." *Structures*, Vol. 9, pp. 13-20, DOI: 10.1016/j.istruc.2016.07.001.

Ronald, Z. D. (2010). *Guide to stability design criteria for metal structures*, Sixth Edition, John Wiley and Sons, Inc., Canada.

Shekastehband, B., Taromi, A., and Abedi, K. (2017). "Fire performance of stiffened concrete filled double skin steel tubular columns." *Fire Safety Journal*, Vol. 88, pp. 13-25, DOI: 10.1016/j.firesaf.2016. 12.009.

Sulthana, U. and Jayachandran, S. (2017). "Axial compression behaviour of long concrete filled double skinned steel tubular columns." *Structures*, Vol. 9, pp. 157-164, DOI: 10.1016/j.istruc.2016.12.002.

Tao, Z., Han, L.-H., and Wang, Z.-B. (2005). "Experimental behaviour of stiffened concrete-filled thin-walled Hollow Steel Structural (HSS) stub columns." *Journal of Constructional Steel Research*, Vol. 61, No. 7, pp. 962-983, DOI: 10.1016/j.jcsr.2004.12.003.

Tao, Z., Han, L. H., and Wang, D. Y. (2007). "Experimental behaviour of concrete-filled stiffened thin-walled steel tubular columns." *Thin-Walled Structures*, Vol. 45, No. 5, pp. 517-527, DOI: 10.1016/j.tws.2007.04.003.

Tao, Z., Han, L.-H., and Wang, D.-Y. (2008). "Strength and ductility of stiffened thin-walled hollow steel structural stub columns filled with concrete." *Thin-Walled Structures*, Vol. 46, No. 10, pp. 1113-1128, DOI: 10.1016/j.tws.2008.01.007.

Tao, Z., Uy, B., Han, L.-H., and Wang, Z.-B. (2009). "Analysis and design

of concrete-filled stiffened thin-walled steel tubular columns under axial compression." *Thin-Walled Structures*, Vol. 47, No. 12, pp. 1544-1556, DOI: 10.1016/j.tws.2009.05.006.

Wang, Z.-B., Tao, Z., and Yu, Q. (2017). "Axial compressive behaviour of concrete-filled double-tube stub columns with stiffeners." *Thin-Walled Structures*, Vol. 120, pp. 91-104, DOI: 10.1016/j.tws.2017.08.025.

Wei, S., Mau, S., Vipulanandan, C., and Mantrala, S. (1995). "Performance of new sandwich tube under axial loading: Analysis." *Journal of Structural Engineering*, Vol. 121, No. 12, pp. 1815-1821, DOI: 10.1061/(ASCE)0733-9445(1995)121:12(1815).

Yang, Z., Li, G., Lang, Y., and Fang, C. (2017). "Flexural behavior of high strength concrete filled square steel tube with inner CFRP circular tube." *KSCE Journal of Civil Engineering*, Vol. 21, No. 7, pp. 2728-2737, DOI: 10.1007/s12205-017-0579-9.

Yu, M., Zha, X., Ye, J., and Li, Y. (2013). "A unified formulation for circle and polygon concrete-filled steel tube columns under axial compression." *Engineering Structures*, Vol. 49, pp. 1-10, DOI: 10.1016/j.engstruct.2012.10.018.

Zhang, Y., Huang, Y., Lei, K., Pei, J., and Zhang, Q. (2017). "Seismic behaviors of steel bar reinforced joints of concrete filled steel tubular laminated columns." *KSCE Journal of Civil Engineering*, Vol. 22, No. 9, pp. 1-13, DOI: 10.1007/s12205-017-0685-8.

Zhao, X.-L. and Grzebieta, R. (2002). "Strength and ductility of concrete filled double skin (SHS inner and SHS outer) tubes." *Thin-Walled Structures*, Vol. 40, No. 2, pp. 199-213, DOI: 10.1016/S0263-8231(01)00060-X.

Zhu, A., Zhang, X., Zhu, H., Zhu, J., and Lu, Y. (2017). "Experimental study of concrete filled cold-formed steel tubular stub columns." *Journal of Constructional Steel Research*, Vol. 134, pp. 17-27, DOI: 10.1016/j.jcsr.2017.03.003.